Short Communication

Electrochemical Machining of Titanium Alloy Based on NaCl Electrolyte Solution

Yafeng He[1,3*], Jianshe Zhao[3]，Huaxing Xiao[1],Wenzhuang Lu[3], Weiming Gan[1,2],
Feihong Yin[1], Zhenwen Yang[3]

[1] Department of Mechanics and Vehicle, Changzhou Institute of Technology, Changzhou 213002, P. R. China
[2] Special Processing Key Laboratory of Jiangsu Province, Changzhou 213002, P. R. China
[3] Nanjing University of Aeronautics and Astronautics, Jiangsu Key Laboratory of Precision and Micro-Manufacturing Technology, Nanjing 210016, P. R. China
[*]E-mail adresses: heyf@czu.cn

Titanium alloy Ti6Al4V is frequently used in the aerospace and other industries. In order to attain Ti6Al4V with a high surface quality, the present study examined the use of side-flow electrochemical machining, paying particular attention to the relationship between the feed rate and the average processing current, balance gap, and surface roughness. Using electrochemical machining channel design and analysis, the surface topographies of titanium alloys, electrochemically machined with different current densities, were investigated. The results showed that, with increasing feed rate, the average processing current increases linearly, while the surface roughness decreases rapidly. When the feed rate is increased to 1.8 mm/min, the balance gap is very small; thus, there is a risk of short-circuit. Simultaneously, with a rapid rise in the current density, the amount of corrosive pitting increased, with the area covered gradually expanding until the activation sites joined together and overlapped each other. Thus, the surface quality of the titanium alloy improved.

1. INTRODUCTION

Titanium alloy Ti6Al4V is widely used in the aerospace and other fields because of its high specific strength, good mechanical properties, and corrosion resistance, making it an ideal material for manufacturing aircraft engine parts. Thus, it has been the subject of considerable research and could be adopted for a wider range of applications [1]. However, owing to its low thermal conductivity and high chemical activity, the cutting tools used to process titanium experience serious wear in the machining processes, which greatly affects the cost performance of the titanium alloy. Non-traditional machining

methods include electrochemical machining, which require a lossless tool cathode, non-application of cutting force, and non-dependence on the material properties, and can thus be used to obtain suitable and effective means of processing titanium alloy. In recent years, the electrochemical machining of titanium alloy has attracted the attention of researchers around the world, leading to several important developments. Mishra et al. proposed electrochemical milling method as a tool to control the movement along a predefined path and it involves a multi-downward step. "L"-shaped features were machined on Ti6Al4V using three different electrolytes by varying their feed rates and frequency and then their corresponding effects on various performance characteristics were studied [2]. The surface morphology and chemistry of titanium alloys were examined using scanning electron microscopy and energy dispersive X-ray spectroscopy. TiO_2 nanotubes were further characterized by cyclic potentiodynamic polarization tests and electrochemical impedance spectroscopy [3]. Klocke investigated the unpulsed electrochemical machinability of four typical TiAl-based alloys. Therefore, the removal rate of specific materials is investigated as a function of current density and their theoretical dissolution behavior was investigated using Faraday's law [4]. Holstein proposed an M-ECM method to obtain the needed accuracy in tungsten microstructure. The achieved progress and observed correlations of processing parameters will be manifested by produced demonstrators made [5]. Laboulais described the passivation behavior of new beta-titanium alloys obtained by powder metallurgy using different electrochemical techniques as well as the existing theoretical models for oxide film growth [6]. An experimental study of the blisk electrochemical machining of titanium alloy was conducted by Chen et al., who attained a high blisk processing quality by optimizing the parameters [7]. An electrochemical machining material removal model for aviation parts was established by Klocke et al., who devised a method of cathode design [8]. Lohrengel et al. examined the dissolution mechanism of the electrochemical machining of titanium alloy and established an inherent law [9,10]. Because of the characteristics of titanium alloy, electrochemical machining can be used to attain passivation; however, this requires a uniform flow field design and selection of reasonable processing parameters to attain high levels of machining accuracy and surface quality. The present study adopted an electrochemical machining method based on a side flow. An experiment was designed for electrolytic machining of Ti6Al4V titanium alloy by the flow and an experiment involving the electrochemical machining of Ti6Al4V titanium alloy in a NaCl electrolyte was conducted for attaining a high-quality processed titanium alloy surface, which could act as a reference for the electrochemical machining of titanium alloy.

2. EXPERIMENTAL

2.1 Principle of side-flow electrochemical machining

To study the surface quality that can be attained by the electrochemical machining of titanium alloy, an electrolyte side flow was adopted for our experiments. The working principle of this technique is shown in Fig. 1. The tool cathode is stationary and is connected to the negative side of a pulse power supply, while the titanium alloy specimens are connected to the positive side. The electrolyte flows through the gap between the tool cathode and titanium alloy specimens at high speed. As the power is increased, the titanium alloy workpiece moves towards the tool cathode at a certain

speed. At the same time, electrochemical reaction and dissolution occur, thus attaining the machining of the titanium alloy surface.
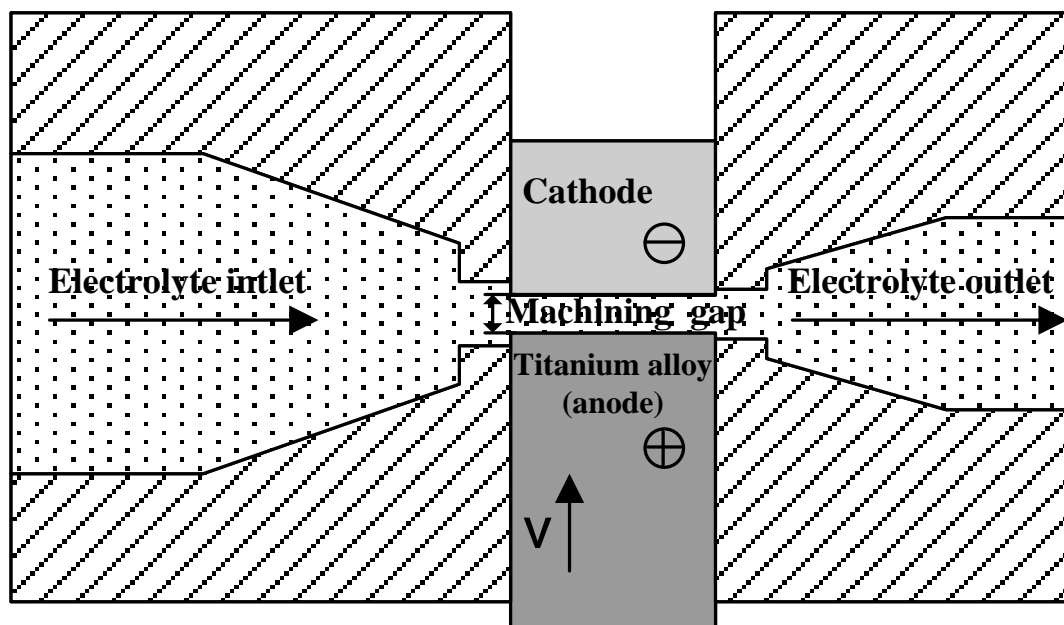

Figure 1. Side-flow electrochemical machining of titanium alloy

2.2 Design of side-flow electrochemical machining

To attain a high-quality machined titanium alloy surface and a high level of precision, the electrolyte flow must attain a specific level of flow field uniformity and stability to avoid the formation of a vortex area and prevent the electrolytic separation phenomenon. To this end, the electrolyte flow in and out of the machining gap, before and after the guide section of the flow channel of the side-flow electrochemical machining, was designed. The streamline distribution flow transition at the rounded corners indicated that the use of a convergent flow from the entrance to the machining gap can improve the electrochemical machining accuracy and stability, as shown in Fig. 2.
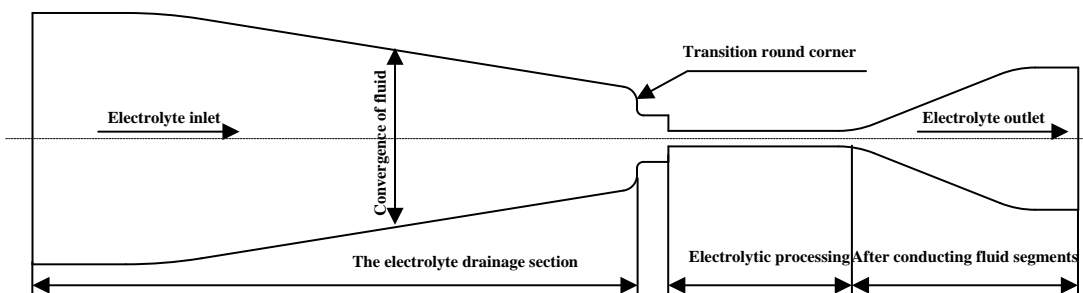

Figure 2. Flow channel of side-flow electrochemical machining of titanium alloy

2.3 Analysis of side-flow electrochemical machining

2.3.1 Flow field model of side-flow electrochemical machining

According to the Reynolds number, the processing clearance flow field of the side-flow electrochemical machining of titanium alloy is turbulent. The mathematical model of the turbulence is as follows:

$$
\begin{cases}
\rho(u \cdot \nabla)u = \nabla \cdot \left[-\rho l + (\mu + \mu_T)\left(\nabla u + (\nabla u)^T\right) \right] + F \\[2mm]
\rho(u \cdot \nabla)k = \nabla \cdot \left[\left(\mu + \dfrac{\mu_T}{\sigma_k}\right)\nabla k \right] + P_k - \rho\varepsilon \\[2mm]
\rho(u \cdot \nabla)\varepsilon = \nabla \cdot \left[\left(\mu + \dfrac{\mu_T}{\sigma_\varepsilon}\right)\nabla\varepsilon \right] + C_{c_1}\dfrac{\varepsilon}{k}P_k - C_{c_2}\rho\dfrac{\varepsilon^2}{k} \\[2mm]
\mu_T = \rho C_\mu \dfrac{k^2}{\varepsilon} \\[2mm]
P_k = \mu_T\left[\nabla u : \left(\nabla u + (\nabla u)^T\right) \right]
\end{cases}
\tag{1}
$$

where u is the liquid phase velocity (m/s), P is the pressure (pa), ρ is the liquid density (kg/m³), F is the increase in the volume force (N/m³), μ is the liquid kinetic viscosity (Pa·s), μ_T is the turbulent viscosity (Pa·s), l is the mixing length, k is the turbulent kinetic energy, ε is the turbulent dissipation rate, and $C_{c1}, C_{c2}, \sigma_k,$ and σ_ε are turbulence coefficients.

2.3.2 Velocity distribution of side-flow electrochemical machining

The aim of the flow design in electrolytic machining is to ensure that the machining gap flow field is uniform and stable. Figure 3 shows the velocity distribution obtained by an analysis for a mass fraction of 10% NaCl electrolyte and an inlet pressure of 0.5 MPa. As shown in the figure, the flow velocity in the passageway is evenly distributed in the processing zone, while there is no electrolyte vortex area between the inlet and outlet, which ensures the quality of electrochemical machining and avoids short-circuits and burning.
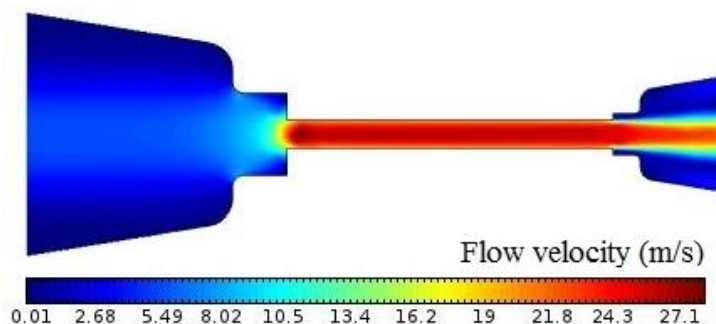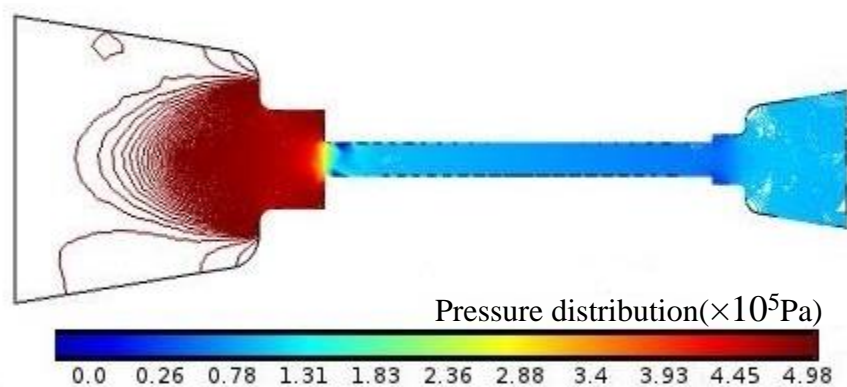

Figure 3. Velocity distribution of side-flow electrochemical machining

2.3.3 Pressure distribution of side-flow electrochemical machining

On the one hand, the electrochemical machining inlet pressure determines the speed that the electrolyte flows through the machining gap. On the other hand, it needs to overcome the viscous friction resistance of the fluid in the machining gap. Owing to the sudden constriction of the flow channel at the machining gap, the velocity of the electrolyte increases. As a result, electrolyte gasification may occur, making it necessary to be aware of any change in the flow pressure. Figure 4 shows the change in the pressure distribution of the entire flow channel for an electrolyte inlet pressure of 0.5 MPa. The graph shows that maintaining a constant pressure in the machining gap is advantageous to electrochemical machining.

Pressure distribution($\times 10^5$Pa)

| 0.0 | 0.26 | 0.78 | 1.31 | 1.83 | 2.36 | 2.88 | 3.4 | 3.93 | 4.45 | 4.98 |

Figure 4. Pressure distribution of side-flow electrochemical machining

3. RESULTS AND DISCUSSION

3.1 Processing parameters for testing of side-flow electrochemical machining

Given the properties of the titanium alloy, a 10% NaCl electrolyte was chosen. Due to the high breakdown voltage during the electrochemical machining of titanium alloy, the processing pulse power average voltage was set to 18 V, while the initial processing gap was 0.6 mm. To attain a uniform machined surface on the titanium alloy, the temperature of the electrolyte was maintained at about 40 °C.

3.2 Test platform for side-flow electrochemical machining

The test platform setup was designed according to the characteristics of side-flow electrochemical machining and based on the preliminary design and analysis of the flow channel (Fig. 5). The titanium alloy specimens are square and are connected to the spindle bar, which is connected to the anode of the pulse power supply. The tool remains stationary and is connected to the cathode of the pulse power supply cathode. Electrochemical machining is completed by feeding the titanium, such that the amount of material removed is determined by the feed rate of the titanium alloy.

The feed rate is an important process parameter affecting the electrochemical machining of titanium alloy and directly affects the machining efficiency and surface quality. The smoothness of electrochemical machining depends on whether a balance can be attained between the feed rate and the anodic dissolution speed, making these the most critical process parameters affecting electrochemical machining.

Figure 5. Test platform for side-flow electrochemical machining

3.3 Influence of feed rates on average processing current

According to Faraday's law, the speed at which the titanium alloy material dissolves in unit time depends mainly on the average processing current. As the average current increases, so too does the anode electrochemical reaction dissolution. Figure 6 shows the change in the average current during processing as the feed rate is changed, while the other conditions remain unchanged. The figure shows that different change trends of the average current during processing arise as the processing progresses and the average current during processing decreases and finally stabilizes as the processing time elapses while the feed rate is low. The average processing current increases with the feed rate after initially decreasing, and then gradually stabilizes as time elapses when the feed rate is relatively high. Due to the use of a linear NaCl electrolyte in the test, as the feed rate increases, the processing average current fluctuates considerably, but overall, it tends to present a linear growth trend.
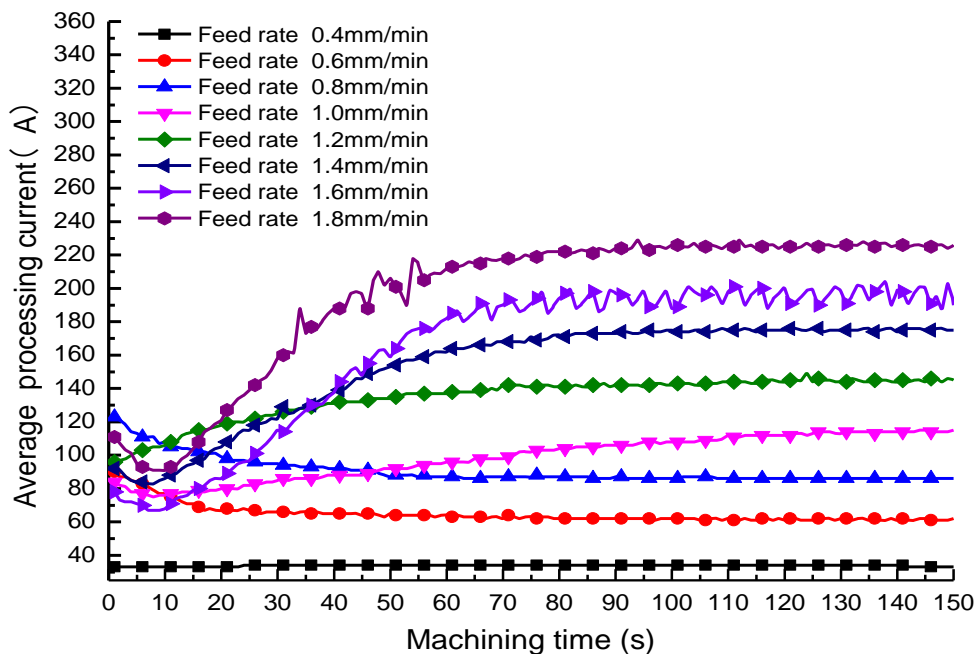
Figure 6. Influence of feed rate on average processing current

3.4 Influence of feed rate on surface roughness

Surface roughness is an important performance index for measuring the processing quality. Figure 7 shows how the roughness of the titanium alloy surface varies as a result of changing the feed rate while keeping all the other conditions unchanged. The figure shows that, as the feed rate increases, the surface roughness tends to reduce rapidly. As the feed rate increases, so too does the surface quality.
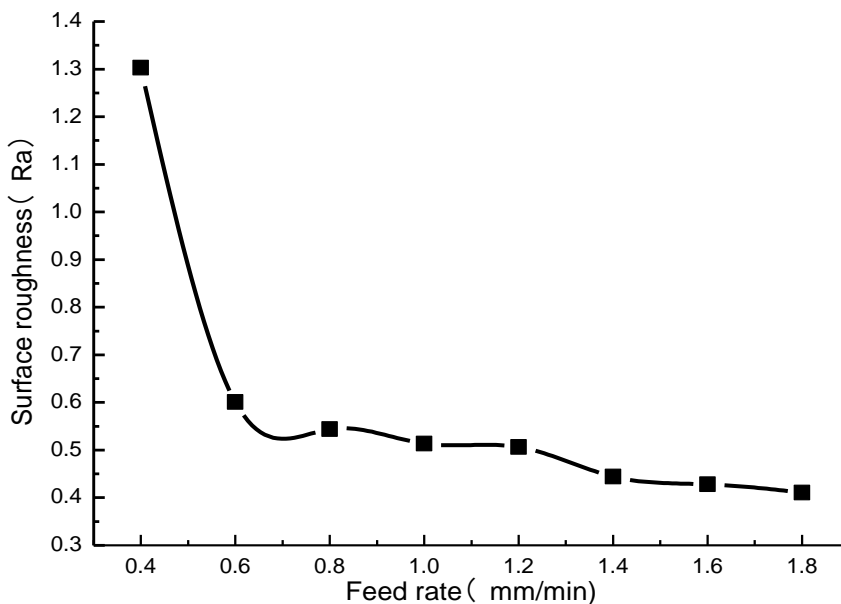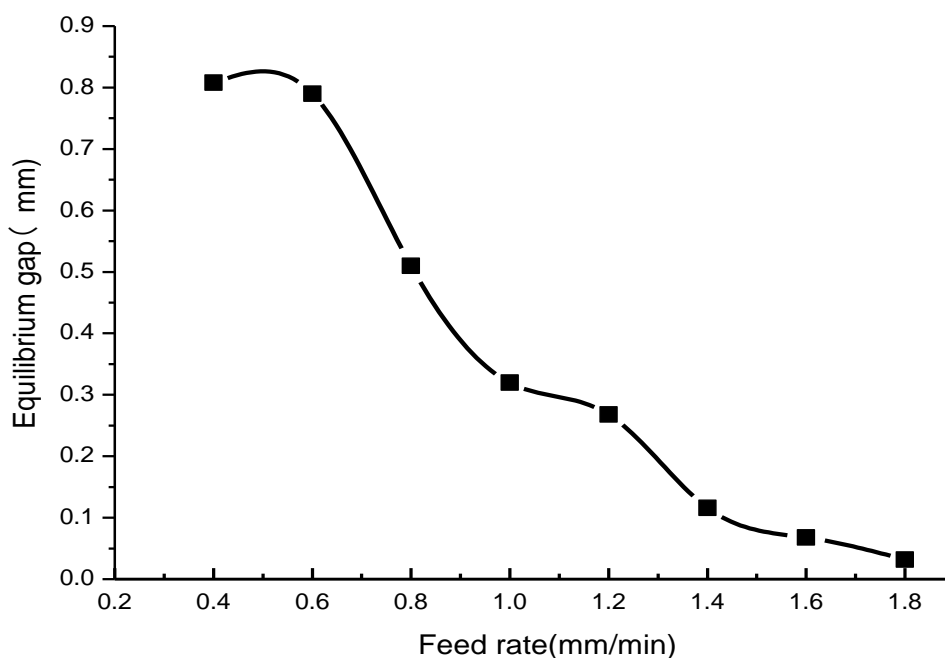

Figure 7. Influence of feed rate on surface roughness

3.5 Influence of feed rate on balance gap

Due to the anode constantly dissolving as a result of the electrochemical reaction that is central to electrochemical machining, the machining gap changes continuously, ultimately tending toward a stable value and forming a balance gap. The processing will fail if a balance is not attained by the end of machining. The balance gap can be measured as described here: first, the coordinates of the end point of the processing tool cathode are recorded, and then the movement of the NC machine tool axis is controlled to make the cathode specimen move, using a multimeter to detect when the tool cathode comes into contact with the specimen, at which point the cathode position coordinates are recorded. Then, the equilibrium gap can be obtained by changing the position coordinates of the cathode. Figure 8 shows the change in the balance gap obtained by changing the feed rate, while keeping all the other conditions unchanged. As the feed rate is increased, the balance gap gradually decreases. For a feed rate of up to 1.8 mm/min, the balance gap is very small, such that a short-circuit or an interruption in the process could occur if the feed rate were to continue increasing.


Figure 8. Influence of feed rate on balance gap

3.6. Surface topography of titanium alloy subjected to side-flow electrochemical machining

Ti6Al4V titanium alloy, which has a high self-passivity, easily reacts with oxygen, generating a passivating film on the alloy surface. Given the high resistance of this passivating film, a barrier layer is formed in the electrochemical machining system, which makes the electrochemical machining of the titanium alloy difficult. Therefore, a NaCl electrolyte with high activity is generally used in the electrochemical machining of titanium alloys, leading to the corrosive pitting of the titanium alloy by

the adsorption of local Cl^- ions, rather than oxygen adsorption. Figure 9 shows that the surface morphologies of the titanium alloy differ considerably depending on the current density, while the Cl^- ions in the electrolyte, depending on the degree of activation, destroy the weak oxygen binding zone of the titanium alloy during processing.
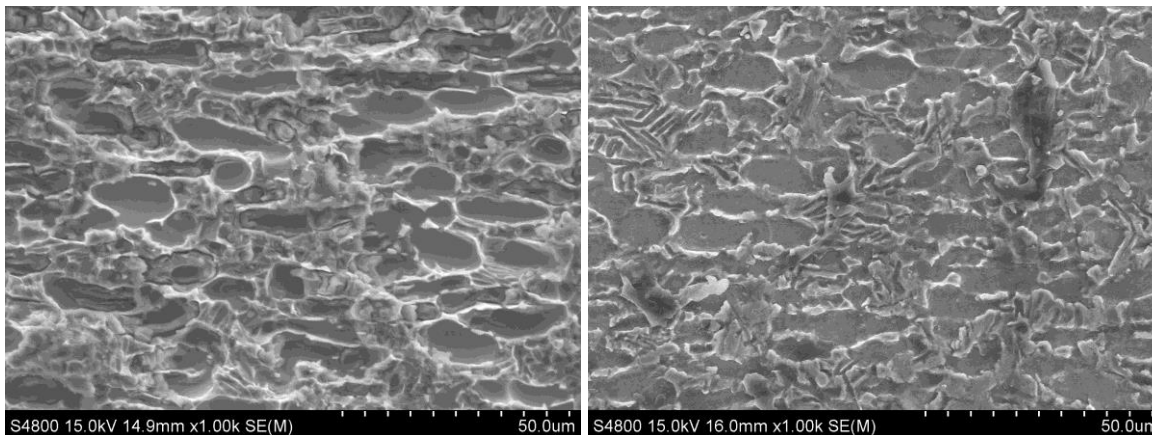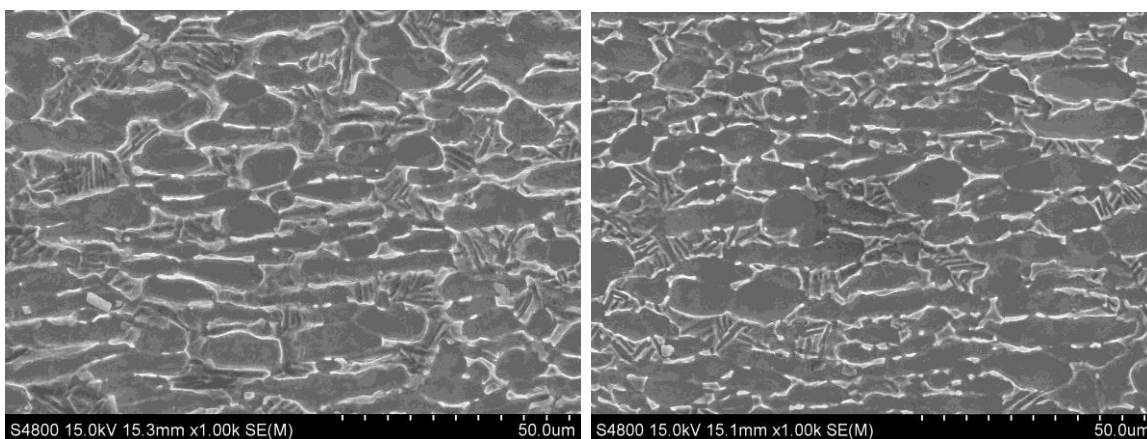

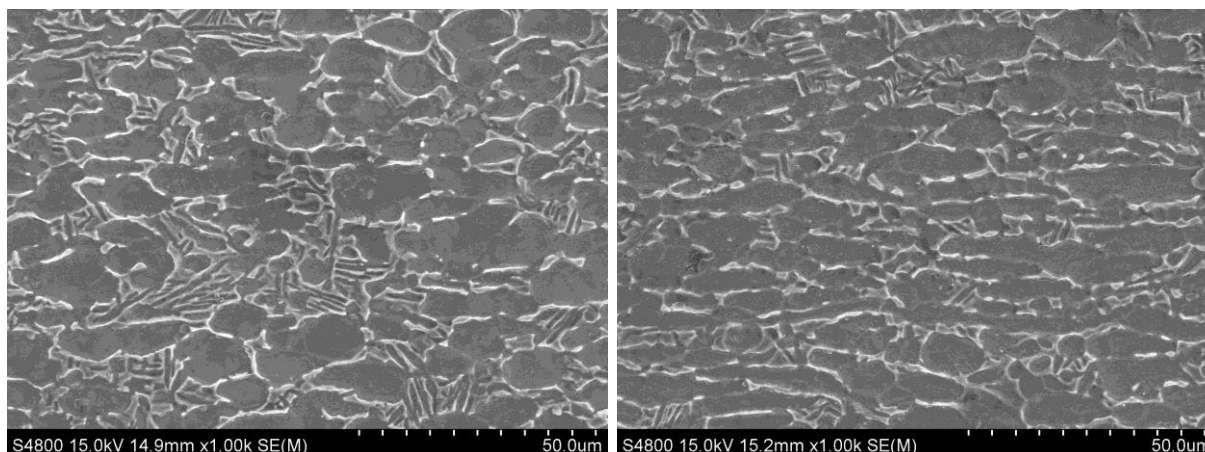(a) Current density = 16 A/cm^2 (b) Current density = 29 A/cm^2
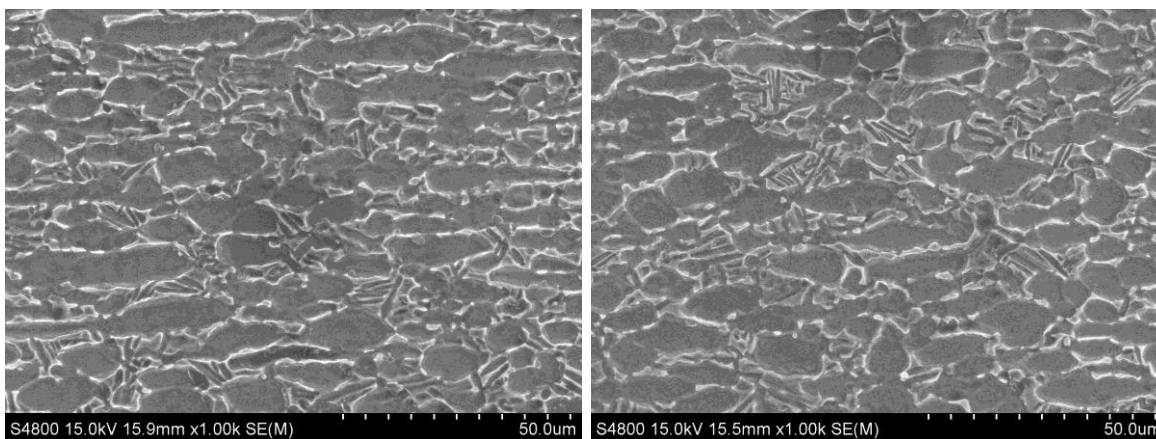
(c) Current density = 42.5 A/cm^2 (d) Current density = 57.5 A/cm^2

(e) Current density = 72.0 A/cm^2 (f) Current density = 88.0 A/cm^2

(g) Current density = 100 A/cm^2 (h) Current density = 112.5 A/cm^2

Figure 9. Dependence of surface topography of titanium alloy on current density

The corrosive pitting mainly occurs in the activation zone of the titanium alloy surface at a low current density of 16 A/cm^2, with the corrosive pitting holes being concentrated and obvious. Figures 9 (b) to (f) show that, as the current density increases from 29 A/cm^2 to 88 A/cm^2, the amount of corrosive pitting on the surface of the titanium alloy increases and the area of corrosive pitting gradually expands. Figures 9 (g), (h) show that, as the current density increases from 100 A/cm^2 to 112.5 A/cm^2, the surface activation site of titanium alloy becomes larger, such that corrosive pitting connects and overlaps, thus making the processed surface smooth and attaining a high processing quality.

Increasingly more attention is being paid to the surface quality of titanium alloy Ti6Al4V processed by electrochemical machining. The formation of the surface of titanium alloy has been examined by researchers, particularly in terms of electrolyte selection, theory analysis, and experimental study [11,12]. For example, surface finish, material removal rate, and pit formations using solutions of sodium halides (bromide, chloride, and fluoride, respectively) are compared with those obtained using the more commonly used sodium nitrate solution. Sodium chloride machining is shown to increase the mass removal rates by over 100% at concentrations of less than 2.5 M, compared with that achievable using the commonly used sodium nitrate electrolyte [13]. Zhu proposed an electrochemical means of drilling multiple holes in which the reverse electrolyte flow is achieved for electrolyte extraction, instead of traditional forward electrolyte flow, which often causes poor electrolyte flow conditions and, therefore, unstable machining [14]. A special procedure for the fabrication of complex microgeometries and microstructured surfaces will be investigated in a future study. This will be done using a continuous electrolytic free jet. A characteristic of this technology is that the electrical current is restricted to a limited area by the jet. Thereby, high localization of the removal area is obtained, which can be easily controlled by changing the current and the nozzle position [15,16,17]. The anodic film growth on Ti alloys in water- and fluoride-containing ethylene glycol electrolyte was investigated by Bojinov, using electrochemical and surface analytical techniques [18], and some improvement in the quality of the titanium alloy processing was reported. Nevertheless,

there is still a need for in-depth investigations because of the characteristics of the titanium alloy and its electrolyte sensitivity. The present study adopted side-flow electrochemical machining as a means of determining the influence of the process parameters of the electrochemical machining process, revealing the evolution of the pitting of titanium alloy in a NaCl electrolyte, thus further improving the quality and accuracy.

4. CONCLUSIONS

1. Titanium alloys are easily passivated during electrochemical machining, but the use of an active NaCl electrolyte ensures the smooth progress of the processing.

2. Flow design and analysis of the electrochemical machining are necessary to ensure machining gap flow field uniformity and stability. The flow passage should be designed with anterior and posterior drainage sections, with a fillet being used where flow transition occurs.

3. As the feed rate increases during processing, so too does the average current, as does the speed at which the titanium alloy dissolves. This increases the efficiency, and produces a better surface roughness and a smaller balance gap. However, if the balance gap were to be allowed to become too small during electrochemical machining, it would lead to serious problems such as short-circuits. In other words, the average current cannot be allowed to exceed an upper limit during the processing, making it vital that a reasonable feed rate be selected to ensure normal processing and surface quality.

4. Corrosive pitting of the titanium alloy can occur easily at low current densities. As the current density increases rapidly, so too does the amount of corrosive pitting. As the area of the corrosive pitting increases, the activation sites connect and overlap. Thus, the surface quality of the titanium alloy improves.

References

1. M. Ahmadi, Y. Karpat, O. Acar, Y. E. Kalay, *J. Mater. Process. Technol.*, 252 (2018) 333.
2. K. Mishra, D. Dey, B. R. Sarkar, B. Bhattacharyya, *J. Manuf. Process*, 29 (2017) 113.
3. Z. U. Rahman, W. Haider, L. Pompa, K. M. Deen, *Mater. Sci. Eng.: C*, 58 (2016) 160.
4. F. Klocke, T. Herrig , M. Zeis , A. Klink, *Procedia CIRP*, 35 (2015) 50.
5. N. Holsteina, W. Krauss, J. Konys, S. Heuer, T. Weber, *Fusion Eng. Des.*, 109 (2016) 956.
6. J. N. Laboulais, A. A. Mata, V. A. Borrás, A. I. Muñoz, *Electrochim. Acta*, 227 (2017) 410.
7. X. Z. Chen, Z. Y. Xu, Z. D. Fang and D. Zhu, Chin, *J. Aeronaut.,* 29 (2016) 274.

8. F. Klocke, M. Zeis, S. Harst, A. Klink and D. Veselovac, *Procedia CIRP*, 8 (2013) 265.
9. M. M. Lohrengel, K. P. Rataj and T. Münninghoff, *Electrochim. Acta*, 201 (2016) 265.
10. D. Baehre, A. Ernst, K. Weißhaar, H. Natter, M. Stolpe and R. Busch, *Procedia CIRP*, 42 (2016)137.
11. W. Liu, S. Ao, Y. Li, Z. Liu, H. Zhang, S. M. Manladan, Z. Luo and Z. P. Wang, *Electrochim. Acta*, 233 (2017) 190.
12. J. Mitchell-Smith and A. T. Clare, *Procedia CIRP*, 42 (2016) 379.
13. A. Speidela, J. Mitchell-Smith, D. A. Walsh, M. Hirsch and A. Clarea, *Procedia CIRP*, 42 (2016) 367.
14. D. Zhu, W. Wang, X. L. Fang, N. S. Qu and Z. Y. Xu, *Cirp Annals – Manuf. Technol*., 59 (2010) 239.
15. M. Hackert-Oschätzchena, G. Meichsner, M. Zinecker, A. Martin and A. Schubert, *Precis. Eng.*, 36 (2012) 612.
16. M. Hackert-Oschätzchena, A. Martin, G. Meichsner, M. Zinecker and A. Schubert, *Precis. Eng.,* 37 (2013) 621.
17. H. Zhang and J. W. Xu, Chin. *J. Aeronaut*., 23(2010) 454.
18. M. Bojinov and M. Stancheva, *J. Electroanal. Chem*., 737 (2015) 150.